Title
Exotic Containers for Capillary Surfaces

Journal
Journal of Fluid Mechanics, 224

Authors
Concus, P.
Finn, R.

Publication Date
1990-02-01

UC-405
LBL-28476
Preprint

Lawrence Berkeley Laboratory
UNIVERSITY OF CALIFORNIA

Physics Division

Mathematics Department

To be submitted for publication

Exotic Containers for Capillary Surfaces

P. Concus and R. Finn

February 1990

Prepared for the U.S. Department of Energy under Contract Number DE-AC03-76SF00098.

DISCLAIMER

LBL-28476

EXOTIC CONTAINERS FOR CAPILLARY SURFACES *

Paul Concus
Lawrence Berkeley Laboratory
and
Department of Mathematics
University of California
Berkeley, California 94720

and

Robert Finn
Department of Mathematics
Stanford University
Stanford, California 94305

February 1990

* This work was supported in part by the Applied Mathematical Sciences Subprogram of the Office of Energy Research, U.S. Department of Energy, under Contract Number DE-AC03-76SF000098, by the National Science Foundation, and by the National Aeronautics and Space Administration.

EXOTIC CONTAINERS FOR CAPILLARY SURFACES

Abstract

In this paper we discuss "exotic" rotationally-symmetric containers that admit an entire continuum of distinct equilibrium capillary free surfaces. The paper extends earlier work to a larger class of parameters and clarifies and simplifies the governing differential equations, while expressing them in a parametric form appropriate for numerical integration. A unified presentation suitable for both zero and non-zero gravity is given. Solutions for the container shapes are depicted graphically along with members of the free-surface continuum, and comments are given concerning possible physical experiments.

1. Introduction

The free surface of a liquid that partly fills a container under the action of surface and gravitational forces may assume, in general, one of several possible equilibrium configurations. An example for which only one configuration is possible is a vertical homogeneous cylindrical container of general cross-section, with gravity either absent or directed downward into the liquid; if the boundary of the free surface lies entirely on the cylindrical walls, then the surface is determined uniquely by its contact angle and the liquid volume [6]. Examples of other containers can be given for which there exist two or more distinct equilibrium configurations. Our interest here is in certain container shapes having the striking property that there is an entire continuum of equilibrium liquid configurations.

In [4], [5] it is shown that there exist rotationally symmetric containers that permit a continuum of distinct, rotationally-symmetric equilibrium free surfaces, all enclosing the same liquid volume and having the same mechanical energy and contact angle. The special case of zero gravity and contact angle $\pi/2$ is studied in [5], where the authors derive a closed-form solution; the general case is studied in [4]. It is shown further in [2], [4] that the families of symmetric solution surfaces are unstable, in that certain asymmetric deformations yield surfaces with lower energy. In fact, it is possible for such "exotic" rotationally-symmetric containers to have energy-minimizing liquid configurations that are not symmetric.

In the present study we extend to a larger range of parameters, and in a form suitable for numerical integration, the equations given in [4] describing the containers. Con-

currently, the equations are clarified and simplified, and a unified presentation is given suitable for both zero and non-zero gravity. The containers are depicted graphically for a range of gravity accelerations and contact angles of physical interest, along with members of the families of symmetric equilibrium free surfaces.

2. Rotationally symmetric capillary surfaces

Consider a rotationally symmetric container, partly filled with liquid, oriented with its axis of symmetry parallel to a uniform downward-acting gravitational field. A rotationally symmetric equilibrium free-surface of the liquid (or interface between two immiscible liquids) satisfies

$$\frac{1}{r}\frac{d}{dr}(r\sin\psi) = Bu + \lambda, \tag{1}$$

where r is the radial coordinate, u is the height of the surface, ψ is the angle between the horizontal and a meridian of the surface, B is the Bond number, and λ is a parameter that is determined by the geometry and volume constraint [3, Chaps. 2,3]. Here we have taken the spatial variables to be normalized with respect to a characteristic dimension ℓ of the container, so that ℓr and ℓu are the physical lengths. The nondimensional parameter B is given by $B = \rho g \ell^2/\sigma$, where ρ is the density of the liquid (less the density of the vapor or of the other liquid phase adjoining the free surface), g is the gravitational acceleration (positive downward), and σ is the interfacial surface tension. The free surface is to meet the container in a prescribed contact angle γ, $0 < \gamma < \pi$, measured within the liquid (see Fig. 1). We consider the case $B \geq 0$.

As discussed in [3], [4], the totality of solutions of (1) defined in a deleted neighborhood of $r = 0$ is described by a one-parameter family of curves. For convenience in subsequent numerical integration of (1), we take $u = 0$ as the initial height at $r = 0$ (where also $\psi = 0$), corresponding to which the parameter λ is twice the curvature of the meridian at the initial umbilical point $r = 0, u = 0$. We include here, as well as the values $|\psi| \leq \pi/2$, the values $\pi/2 < |\psi| < \pi$, which were not considered in [4].

If $\lambda = 0$, then the solution curve is $u \equiv 0$. As shown in [3], if $\lambda > 0$, then on any solution curve the curvature $k = \frac{d}{dr}(\sin\psi)$ remains positive, increasing monotonically

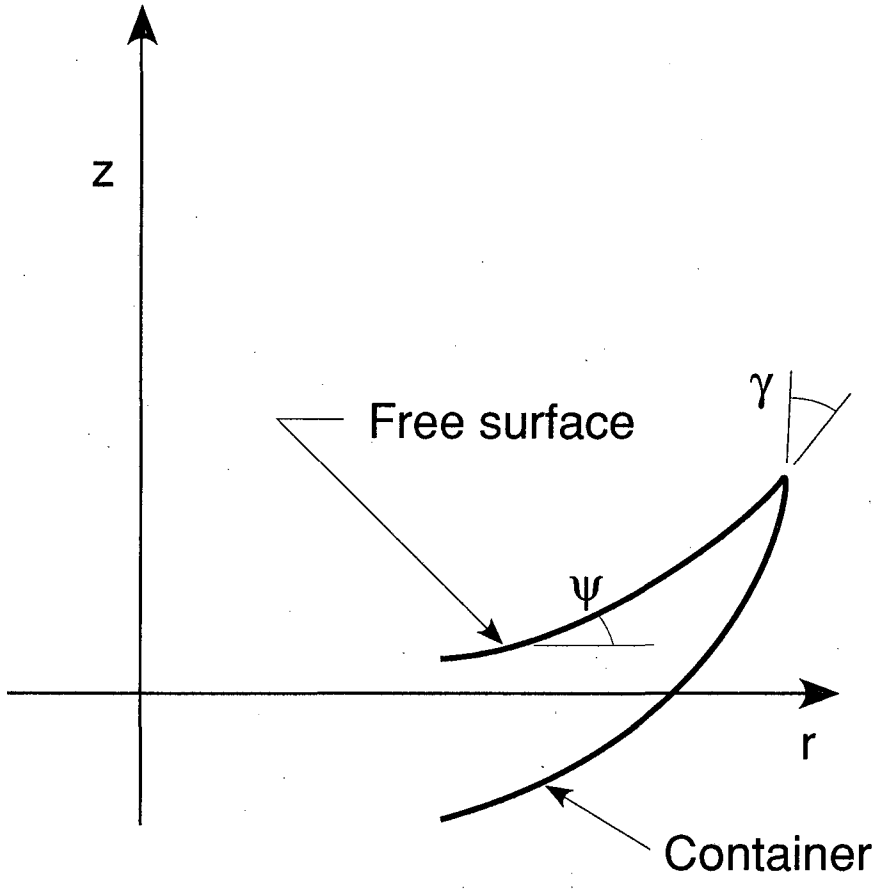

Figure 1

with ψ; correspondingly, u increases monotonically as ψ varies from 0 to π. Similarly, if $\lambda < 0$, then the curvature k remains negative, decreasing monotonically, along with u, as ψ decreases from 0 to $-\pi$.

If $r = R > 0$ and $\psi = \Psi$ are prescribed terminal values of r and ψ, then the parameter λ is determined uniquely by these values. We may denote the unique solution surface as described parametrically in terms of ψ in the region of interest $|\psi| < \pi$ by

$$\begin{aligned} r &= \rho(\psi; R, \Psi) \\ z &= u(\psi; R, \Psi). \end{aligned} \tag{2}$$

The corresponding parametric representation of (1) is

$$\begin{aligned} \frac{d\rho}{d\psi} &= \frac{1}{k}\cos\psi, \\ \frac{du}{d\psi} &= \frac{1}{k}\sin\psi, \end{aligned} \tag{3}$$

where

$$k = Bu - \frac{\sin\psi}{\rho} + \lambda \tag{4}$$

is the curvature of the solution curve. The initial and terminal conditions become

$$\begin{aligned} \rho = u = 0 \ , \ \text{at } \psi = 0 \\ \rho = R, \ \text{at } \psi = \Psi. \end{aligned} \tag{5}$$

If $\Psi = 0$, then the solution of (1) satisfying the prescribed terminal conditions is $u \equiv 0$, for which $k \equiv 0$, and the parametric representation (3) is unsuitable. Otherwise, as discussed above, k cannot vanish and the representation (3) is appropriate.

The terminal values R and Ψ for our numerical integration will be those at which the solution curve meets the container. So that the curve corresponds to the coordinates in which the container is expressed, we shall in what follows displace it vertically, adding a constant h to u, by specifying the value of the displaced surface height $u + h$ at the end point $r = R, \psi = \Psi$. The displaced height remains a solution to (3) (or (1)), with $\lambda - Bh$ replacing λ, and the condition $\psi = \Psi$ at $r = R$ is unchanged.

3. Determination of the containers

As in [4] we seek a rotationally symmetric container given by $r = f(z)$ (which it will be convenient later to describe also in parametric form). The container is to be such that

a family of rotationally symmetric interfaces obtained from solutions to (1), all having the same contact angle, enclose with it the same liquid volume. Let $(R = f(Z), Z)$ denote a point on the container meridian, and at (R, Z) let the value of ψ for the interface solution meridian intersecting the container there be $\psi = \Psi$. Then the volume V enclosed between the free surface and the container is given by

$$V = \frac{2\pi}{B}\left[-(Bu+\lambda)\frac{R^2}{2} + R\sin\Psi\right] + \pi\int^Z R^2 dz, \tag{6}$$

as derived in [4, Eqs.(9) and (10)] using integration of the Bu term in (1) to obtain the volume below the free surface. The equations in [4] were derived with reference only to the case $|\Psi| \leq \pi/2$; however, it can be shown that the expression (6) for V holds over the entire range $-\pi < \Psi < \pi$. By using the asymptotic representation for λ near $B = 0$,

$$\lambda = \frac{2}{R}\sin\Psi + O(B)\ ,\ B \to 0,$$

one obtains from the results in [1] that the expression (6) for V has the limit at $B = 0$ (for which value u is a circular arc of radius $\frac{R}{\sin\Psi}$),

$$V\Big|_{B=0} = -\pi R^3\left[\frac{1-\cos\Psi}{\sin\Psi} - \csc\Psi + \frac{2}{3}\csc^3\Psi(1-\cos^3\Psi)\right] + \pi\int^Z R^2 dz.$$

This expression can be rearranged and simplified to

$$V\Big|_{B=0} = -\pi R^3\frac{\sin\Psi(2+\cos\Psi)}{3(1+\cos\Psi)^2} + \pi\int^Z R^2 dz. \tag{7}$$

This connects the general expression (6) with the expression derived explicitly for $B = 0$ as (7) in [4] and [5].

We turn now to a parametric representation of the container given by $r = R(\phi), z = Z(\phi)$, where ϕ is the angle between the horizontal and a meridian of the container, $\cot\phi = df/dr$. The condition that a solution surface meridian meet the container with prescribed contact angle γ is that

$$\phi - \Psi = \gamma \tag{8}$$

at the point of intersection, see Fig. 2.

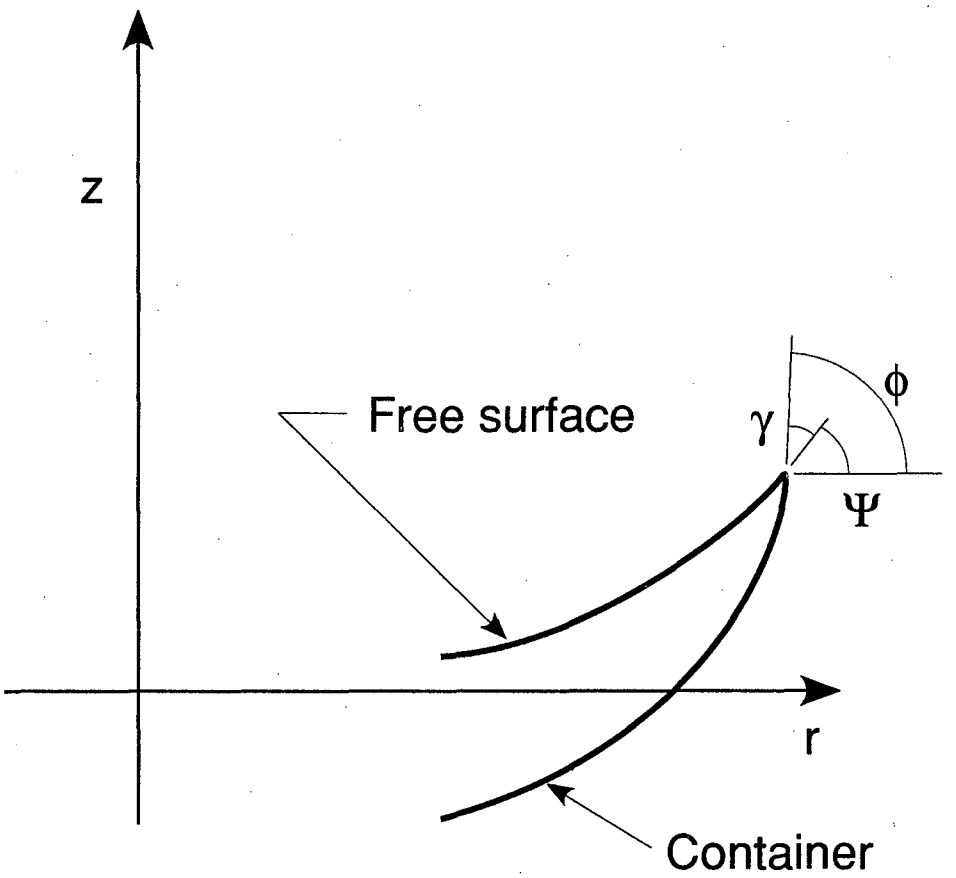

Figure 2

The solution surface $\rho(\psi; R, \Psi), u(\psi; R, \Psi)$, which attains the values $\rho = R, \psi = \Psi$ at the end point, must be displaced vertically upward a distance $h = Z - u(\Psi; R, \Psi)$ to pass through the point (R, Z) (cf., the last paragraph of Sec. 2). Thus the displaced free-surface solution intersecting the container at (R, Z) with angle Ψ is given by

$$u(\psi; R, \Psi) + Z - u(\Psi; R, \Psi).$$

As the condition for constant enclosed volume, we set $\frac{dV}{d\phi} = 0$, obtained by differentiation of (6). Let

$$U(R, \Psi) = u(\Psi; R, \Psi)$$

denote the value of u at the container intersection and $\lambda(R, \Psi)$ the corresponding value of the parameter λ. We shall denote partial differentiation of U or λ with respect to R or Ψ by the corresponding subscript. Finally, let

$$K = BU - \frac{\sin \Psi}{R} + \lambda$$

denote the value at the container intersection of the meridional curvature k of the solution surface, cf. (4). Then, using $\frac{d\Psi}{d\phi} = 1$, we obtain for the condition of constant enclosed volume

$$Q + \frac{2}{B}\left[-\frac{R}{2}(BU_R + \lambda_R) - K\right]\frac{dR}{d\phi} + R\frac{dZ}{d\phi} = 0, \tag{9}$$

where

$$Q = \frac{2\cos\Psi - BR(BU_\Psi + \lambda_\Psi)}{B}. \tag{10}$$

The use of a parametric form in terms of the parameter ϕ for deriving (9), (10), and subsequent equations from (6) and (8) simplifies the corresponding derivation required in [4] for the non-parametric form with r as independent variable.

The partial derivatives of U with respect to R and Ψ are related, since $\frac{du}{dr} = \tan\psi$ along a solution curve. One has

$$\tan\Psi = U_R + U_\Psi \frac{d\Psi}{dR},$$

which yields, using (3),

$$\sin\Psi = U_R \cos\Psi + KU_\Psi. \tag{11}$$

Similarly,

$$\lambda_R \cos\Psi + K\lambda_\Psi = 0. \tag{12}$$

Using these relationships, one obtains from (9) the equation

$$Q\cos\Psi - (KQ + R\sin\Psi)\frac{dR}{d\phi} + R\cos\phi\frac{dZ}{d\phi} = 0. \tag{13}$$

Finally, one can write the above equation in parametric form as

$$\begin{aligned} \frac{dR}{d\phi} &= \frac{\cos\phi}{k_c}, \\ \frac{dZ}{d\phi} &= \frac{\sin\phi}{k_c}, \end{aligned} \tag{14}$$

where k_c, the meridional curvature of the container, is given by

$$k_c = \frac{KQ\cos\phi - R\sin\gamma}{Q\cos\Psi}. \tag{15}$$

The system of equations (14) is the one that we wish to solve to determine the desired container shapes.

4. Properties of container equations

For small values of B, one can use the asymptotic properties of the free surface meridian given in [1, Sec. 3] to obtain from (10) the asymptotic relationship

$$Q = -\frac{R^2}{(1+\cos\Psi)^2} + O(B),\ B \to 0.$$

Thus Q has a limit at $B = 0$ (for all Ψ, $-\pi < \Psi < \pi$). The resulting limit of (13) can be shown to correspond to the governing equations derived separately for the $B = 0$ case in [4] and [5], thus unifying the cases for zero and non-zero B.

The suggestion of singular behavior at $\Psi = \pi/2$, occasioned by the explicit appearance of $\cos\Psi$ in the denominator of (15), is illusory and can be removed by using (8), (10), (11), and (12). One obtains

$$k_c = K\cos\gamma - \frac{1}{Q}\left(\frac{2K\sin\Psi}{B} + R\cos\Psi + R\sin\Psi\left(U_R + \frac{\lambda_R}{B}\right)\right)\sin\gamma.$$

This form is more suitable for computation near $\Psi = \pi/2$ than is (15).

In the numerical integration of (14), which is discussed in the following section, we shall take the initial point to lie on the planar solution surface $u \equiv 0$ of (1), corresponding to $\Psi = 0$, for which $K = 0$. From (15) one obtains that $k_c = \frac{4}{R}\sin\gamma > 0$ at the initial point, since $0 < \gamma < \pi$. Thus the system (14) is well-behaved at the initial point. Nearby, for $|\Psi|$ small, one obtains, using the asymptotic representation of the free surface meridian [1], that

$$K = \lambda\left[I_0(B^{1/2}R) - \frac{I_1(B^{1/2}R)}{B^{1/2}R}\right]\left(1 + O(\Psi^2)\right), \quad \Psi \to 0$$

and that

$$k_c = \left(\frac{B^{1/2}RI_0(B^{1/2}R)}{I_1(B^{1/2}R)} - 1\right)\frac{-\sin\gamma}{R\left(\frac{3I_0(B^{1/2}R)}{B^{1/2}RI_1(B^{1/2}R)} - \frac{2}{BR^2} - \left[\frac{I_0(B^{1/2}R)}{I_1(B^{1/2}R)}\right]^2\right)} \cdot \left(1 + O(\Psi^2)\right).$$

One can show easily, using computer representations for the modified Bessel functions I_0 and I_1, that k_c remains positive away from the initial point. The computed solutions of (14) for the examples we considered indicate that k_c is positive over the entire range $0 \le \phi \le \pi$, increasing with ϕ, and hence that integration of the parametric form (14) can be carried out.

It is shown in [4] that for the case $|\Psi| \le \pi/2$ there holds $Q < 0$. Our numerical solutions for the cases we have considered indicate that Q remains negative and decreases as Ψ increases through the range $-\pi < \Psi < \pi$.

5. Numerical solution

Numerical solutions of (14) were calculated for several values of contact angle γ and Bond number B. The initial values for the integration were $R = 1, Z = 0, \phi = \gamma$, corresponding to the solution surface $u \equiv 0$ of (1), for which $\psi \equiv 0$. Eq. (14) was integrated forward in ϕ to obtain the upper portion of the container $\gamma \le \phi \le \pi$ and backward in ϕ for the lower portion $0 \le \phi < \gamma$. The integration was accomplished by a variable-order variable-step Adams method using subroutine D02CBF of the NAG program library. To evaluate the coefficients at each integration step, a boundary value problem (3), (5) for

the liquid free surface was solved by a shooting method using NAG library subroutine D02HBF.

The necessary quantities in (15) at each integration step were obtained by solving numerically the system

$$\frac{d}{ds}\begin{bmatrix}\rho\\ u\\ \psi\end{bmatrix} = \begin{bmatrix}\cos\psi\\ \sin\psi\\ k\end{bmatrix}, \tag{16}$$

where k is given by (4). At the initial point $s = 0$, at which $\rho = u = \psi = 0$, k has the limiting value $(Bu + \lambda)/2$. The system (16) is equivalent to the system (3), where now arclength s is the independent variable instead of ψ. In return for the extra complication of treating a system of three equations rather than two, more robust behavior was obtained in calculating solutions near the planar one $u \equiv 0, k \equiv 0$, with better error control using the automatic procedure built into the integration subroutine. Appended to the system (16) were the equations for the partial derivatives with respect to R, with ψ and Ψ fixed,

$$\frac{d}{ds}\begin{bmatrix}\rho_R\\ u_R\end{bmatrix} = -\frac{k_R}{k}\begin{bmatrix}\cos\psi\\ \sin\psi\end{bmatrix},$$

$$k_R = Bu_R + \frac{\sin\psi}{\rho^2}\rho_R + \lambda_R.$$

The boundary conditions for the integration for the complete system are

$$\text{at } s = 0: \quad \rho = u = \psi = \rho_R = u_R = 0$$

$$\text{at } s = S: \quad \rho = R,\ \psi = \Psi,\ \rho_R = 1.$$

At the initial point $s = 0$, k_R has the limiting value $(Bu_R + \lambda_R)/2$. These equations determine the four quantities $U = u(S)$, $U_R = u_R(S)$, λ, and λ_R required in (15). The unknown parameter S, the total arclength of the interface, is obtained as part of the numerical integration.

To start the integration from the initial planar interface $u \equiv 0$, the asymptotic form for small ψ given in [1] was used to provide initial values for the Newton iterates for λ_R and $u_R(S)$, based on the Ψ derivatives

$$\left.\begin{aligned}\lambda_\Psi &= \frac{\sqrt{K}}{I_1(\sqrt{K})}\\ u_\Psi(S) &= \frac{\lambda_\Psi}{K}(I_0(\sqrt{K}) - 1)\end{aligned}\right\}, \text{ if } K \neq 0, \qquad \left.\begin{aligned}\lambda_\Psi &= 2\\ u_\Psi(S) &= \frac{1}{2}\end{aligned}\right\}, \text{ if } K = 0.$$

Subsequently the values at the most recent previous integration point of ϕ were used as the initial ones.

In Figs. 3, 4, 5 the solutions calculated for $\gamma = 30°, 60°, 90°$ and $B = 0, 1, 10, 100$ are depicted. (The solutions for the supplementary non-wetting cases $\gamma = 120°$ and $\gamma = 150°$ can be obtained by reflecting, respectively, the $\gamma = 60°$ and $\gamma = 30°$ ones about $z = 0$.) The container meridians are shown as solid curves. For each figure the dashed curves depict meridians of members of the family of symmetric equilibrium free surfaces, all enclosing the same volume, having the same mechanical energy, and meeting the container with the same contact angle. The plotted free-surface curves include the horizontal, planar member of the family and are given for increments of 30° in Ψ. For $\gamma = 0°$ the free surfaces and container would coincide. For some cases, as depicted for the 30° contact-angle curves, only an appropriate portion of the container should be used consistent with the implicit physical requirement that the free surfaces lie interior to the container, intersecting it only at the final integration point. In all cases a top and bottom of the container could be connected to the symmetry axis as desired (provided the connecting portions do not encroach on the free surfaces). Fig. 6 illustrates a container consisting of the entire computed solution for $B = 0$ shown in Fig. 4 connected to circular cylindrical extensions above and below, with disk ends. By joining only a small portion near $\phi = \pi/2$ of a computed container shape to circular cylindrical extensions, one obtains a container that is as close as desired to being a circular cylinder. It would still admit an entire continuum of equilibrium free surfaces, whereas for prescribed contact angle and liquid volume the circular cylinder admits only the unique, symmetric equilibrium surface of minimizing energy if the boundary of the free surface lies entirely on the cylindrical walls.

In the figures the containers are scaled to have maximum radius of unity. Since the Bond number B for the numerical integration is based on a characteristic length ℓ equal to the radius of the flat interface (i.e., $R = 1$), the scaling in the figures corresponds to a scaling of Bond number as well. The scaling factor a is given on each figure. The Bond number based on the maximum-radius characteristic length is Ba^2.

Generally, the figures indicate that as B increases, the containers become more eccentric, and the corresponding solution surface family more compressed. A low-gravity

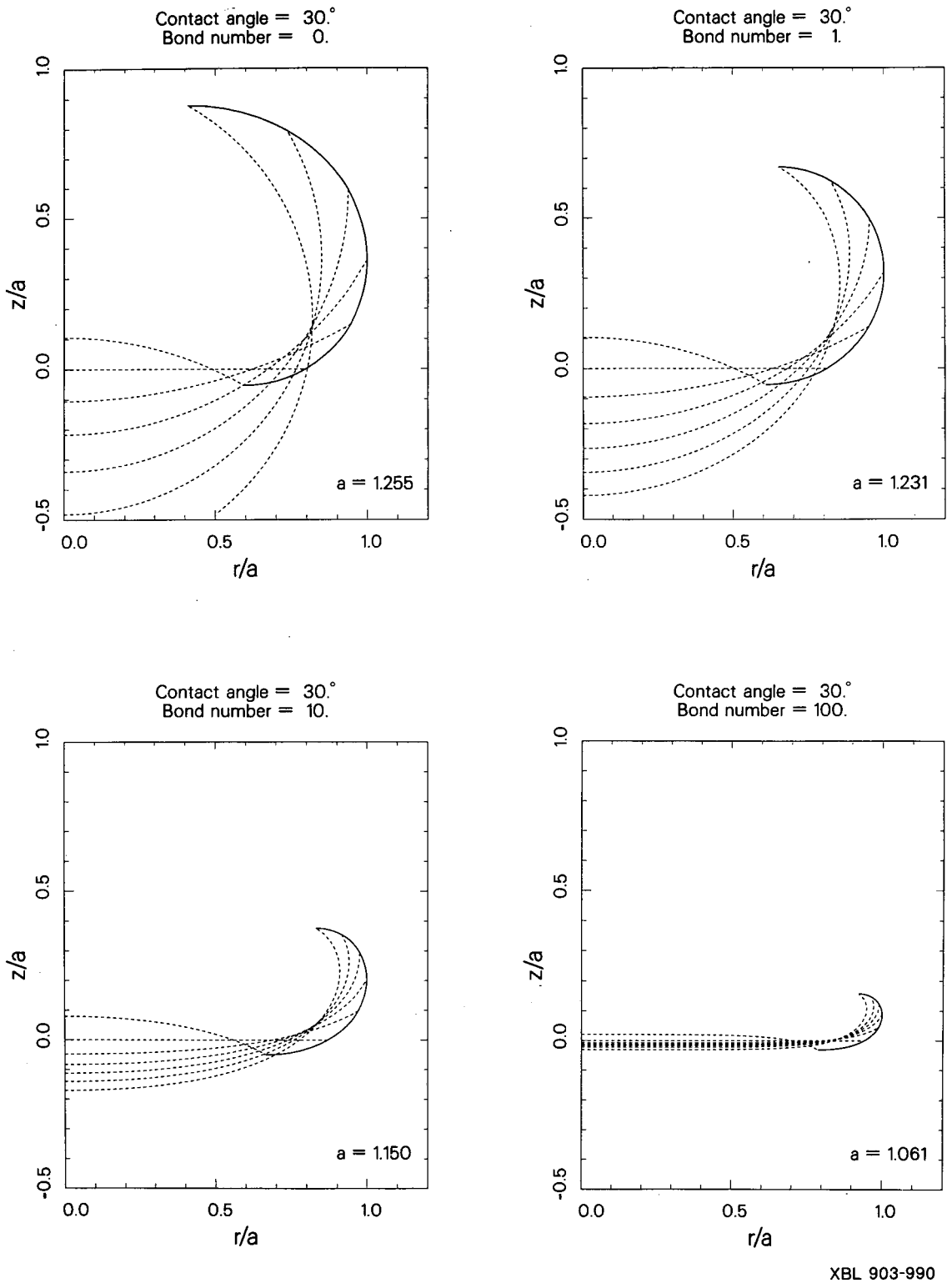

Figure 3. Meridian of container (solid curve) for contact angle 30° and several Bond numbers showing meridians of some symmetric equilibrium solution surfaces (dashed curves), all having the same contact angle and energy, and enclosing the same volume of liquid.

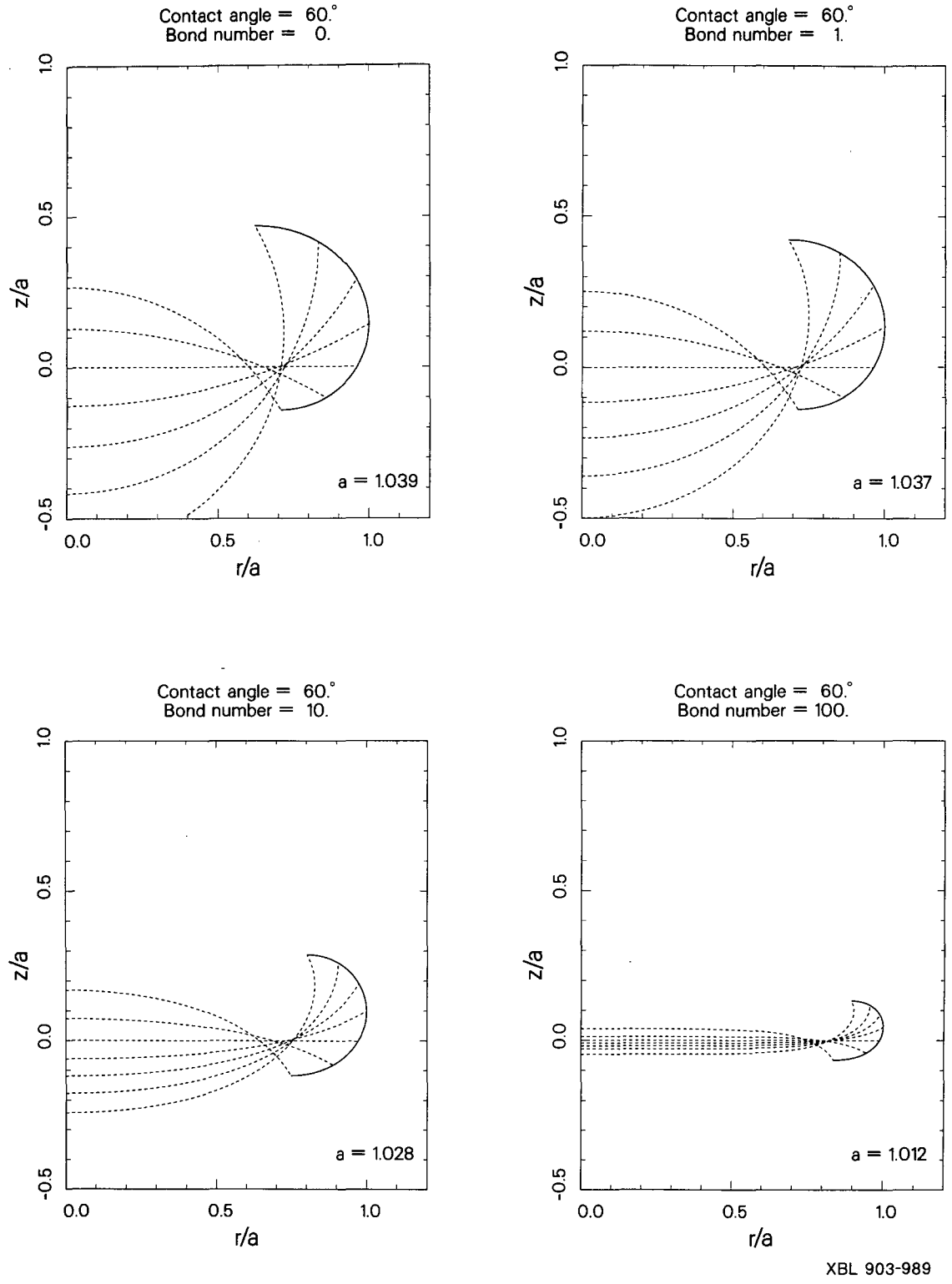

Figure 4. Meridian of container (solid curve) for contact angle 60° and several Bond numbers showing meridians of some symmetric equilibrium solution surfaces (dashed curves), all having the same contact angle and energy, and enclosing the same volume of liquid.

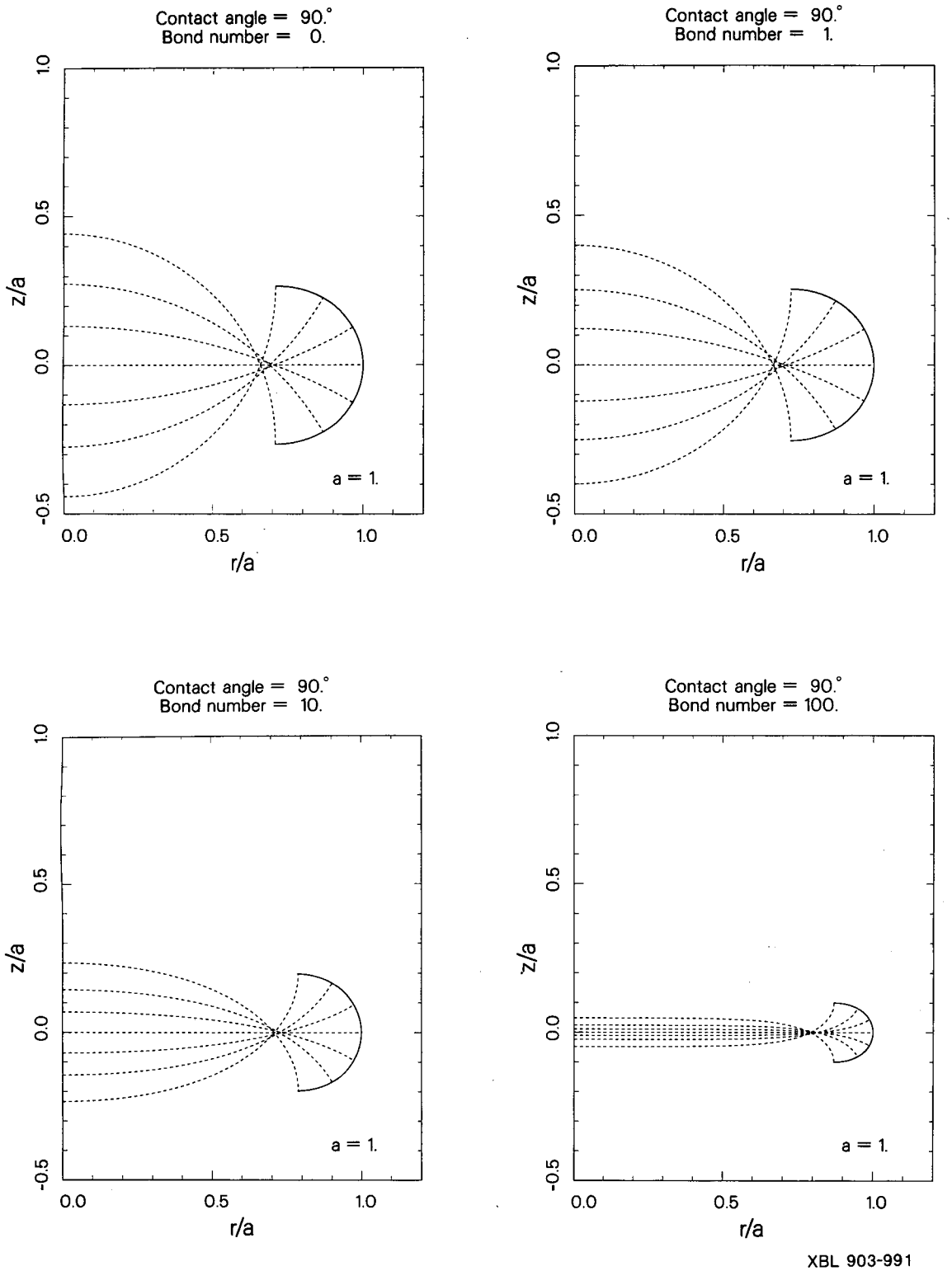

Figure 5. Meridian of container (solid curve) for contact angle 90° and several Bond numbers showing meridians of some symmetric equilibrium solution surfaces (dashed curves), all having the same contact angle and energy, and enclosing the same volume of liquid.

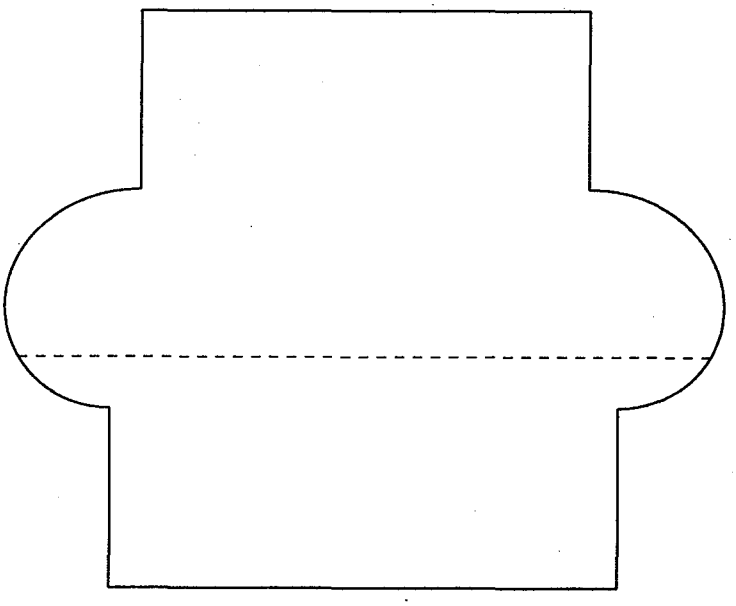

Figure 6. Container for contact angle 60° and $B = 0$ with top and bottom right circular cylindrical extensions and disk ends. The dashed line indicates the fill level corresponding to a planar equilibrium interface.

environment would have substantial advantages for carrying out related physical experiments, since an adequately large length scale for accurate observation and measurement would thereby be permitted.

An initial step in visualizing the physical behavior of liquid in these containers was taken by M. Weislogel at the NASA Lewis Research Center Zero Gravity Facility. Of particular interest for physical experiments is the property shown in [2], [4], that a configuration of lower mechanical energy can be obtained by a non-rotationally-symmetric perturbation of the planar member of the family of solution surfaces. Thus, under the idealized Young-Laplace equilibrium contact-angle conditions embodied by (8), if surface friction effects were absent, the symmetric equilibrium free surfaces, as depicted here, would not be observed physically in the containers.

We wish to thank M. Montgomery for programming some of the computer graphics and M. Miranda for his hospitality while the authors were visiting at Università di Trento, where portions of the manuscript were written.

References

[1] P. Concus, *Static menisci in a vertical right circular cylinder*, J. Fluid Mech. 34 (1968), pp. 481–495.

[2] P. Concus and R. Finn, *Instability of certain capillary surfaces*, Manuscr. Math. (1989), pp. 209–213.

[3] R. Finn, *Equilibrium Capillary Surfaces*, Springer-Verlag, New York, 1986.

[4] R. Finn, *Nonuniqueness and uniqueness of capillary surfaces*, Manuscr. Math. 61 (1988), pp. 347–372.

[5] R. Gulliver and S. Hildebrandt, *Boundary configurations spanning continua of minimal surfaces*, Manuscr. Math. 54 (1986), pp. 323–347.

[6] T. I. Vogel, *Uniqueness for certain surfaces of prescribed mean curvature*, Pacific J. Math. 134 (1988), pp. 197–207.

LAWRENCE BERKELEY LABORATORY
UNIVERSITY OF CALIFORNIA
INFORMATION RESOURCES DEPARTMENT
1 CYCLOTRON ROAD
BERKELEY, CALIFORNIA 94720